Chinese Journal of
POLYMER SCIENCE

RESEARCH ARTICLE

https://doi.org/10.1007/s10118-025-3428-1
Chinese J. Polym. Sci. **2025**, *43*, 2118–2127

Multi-mode Polarized Luminescent Au-nanorod Polymer Composites for Advanced Optical Anti-counterfeiting

Li-Rong Xu[b], Jia-Yong Wang[a], Jin-Ting Huang[a], Qian-Yi He[a], Shao-Lin Lu[a,c*], Deng-Chong Feng[a,c*], Ze-Tong Ma[a,c], Zhong-Ke Yuan[a,c], Yu-Zhao Yang[a,c*], and Xu-Dong Chen[a,b,c]

[a] *School of Chemical Engineering and Light Industry, Guangdong University of Technology, Guangzhou 510006, China*
[b] *Key Laboratory for Polymeric Composite and Functional Materials of Ministry of Education, School of Chemistry, Sun Yat-Sen University, Guangzhou 510275, China*
[c] *Guangdong Provincial Laboratory of Chemistry and Fine Chemical Engineering Jieyang Center, Jieyang 515200, China*

Electronic Supplementary Information

Abstract The development of organic afterglow materials with high environmental stability and multi-mode luminescence remains a significant challenge in luminescent anti-counterfeiting. In this work, an organic luminescent molecule was encapsulated within polyacrylamide microspheres and embedded in a gold nanorod-doped, ferric ion-crosslinked hydrogel exhibiting upper critical solution temperature behavior. The obtained composites exhibited fluorescence, thermally activated delayed fluorescence, and phosphorescence. Through the application of extrusion or uniaxial stretching, the orientation of the gold nanorods was modulated, enabling polarization-dependent luminescence through transverse surface plasmon resonance absorption. At 300% uniaxial strain, the polarized fluorescence intensity difference at 520 nm reached 0.29. Furthermore, ultraviolet irradiation was employed to locally disrupt the orientation of the gold nanorods, resulting in depolarization within the irradiated regions. These areas displayed non-polarized fluorescence, while the non-irradiated regions retained both emission and fluorescence polarization characteristics. Localized imprinting was employed to modulate material thickness, thereby controlling the density of gold nanorods. Thinner regions exhibited weaker transverse localized surface plasmon resonance absorption, while thicker regions showed stronger absorption, enabling the coexistence of blue–green fluorescence and polarization patterns. Local humidification effectively reduced phosphorescence intensity, enhancing the material's environmental responsiveness. The composite demonstrated excellent reversibility over multiple stretching–self-healing cycles and pattern-switching processes, highlighting its strong potential for multidimensional optical encryption and intelligent anti-counterfeiting applications.

Keywords Gold nanorods; Hydrogel polymer; Polarization; Anti-counterfeiting; Luminescence material

Citation: Xu, L. R.; Wang, J. Y.; Huang, J. T.; He, Q. Y.; Lu, S. L.; Feng, D. C.; Ma, Z. T.; Yuan, Z. K.; Yang, Y. Z.; Chen, X. D. Multi-mode polarized luminescent Au-nanorod polymer composites for advanced optical anti-counterfeiting. *Chinese J. Polym. Sci.* **2025**, *43*, 2118–2127.

INTRODUCTION

With the growing demand for high-security applications, anti-counterfeiting technologies that enable dynamic information encryption and multidimensional optical signal regulation are becoming increasingly important.[1–3] Traditional single-mode anti-counterfeiting materials face significant limitations such as high crackability and limited information capacity, which necessitate innovative breakthroughs.[4–6] Organic luminescent materials have attracted considerable attention in the field of optical encryption owing to their diverse excitation–emission properties and high design flexibility.[7–13] In particular, triple-emission systems combining fluorescence, delayed fluorescence, and phosphorescence enable high-level information encryption through the coordinated modulation of multiple parameters, such as emission lifetime, wavelength, and polarization.[14,15] However, such systems still face significant challenges for practical applications. (1) Luminescent molecules are highly susceptible to quenching by environmental water and oxygen, which leads to poor optical stability.[16,17] (2) The independent regulation of multiple luminescence modes remains difficult, making it challenging to achieve a complex dynamic encryption logic.[18] (3) As a critical dimension in optical encryption, the integration of polarized luminescence with multimode emission is often constrained by the limited tunability of material anisotropy and poor adaptability to mechanical deformation.[19] Although efforts have been made to enhance material stability through a rigid matrix encapsulation and energy transfer regulation, an effective strategy for dynamically coupling the emission wavelength, lifetime, and polarization angle under complex environ-

* Corresponding authors, E-mail: lushlin@gdut.edu.cn (S.L.L.)
E-mail: fengdch@gdut.edu.cn (D.C.F.)
E-mail: yangyuzh@gdut.edu.cn (Y.Z.Y.)

Received June 18, 2025; Accepted August 5, 2025; Published online October 16, 2025

mental conditions has yet to be realized.[20–22]

In recent years, linearly polarized luminescent materials have demonstrated unique wavelength-selective absorption characteristics through the controlled orientation of plasmonic resonance units, such as gold nanorods (AuNRs), offering a novel idea for dynamic polarization encryption.[23–25] However, most existing systems mainly focus on polarization modulation of a single luminescence mode and often depend on complex liquid crystal templates or external field alignment techniques, which hinder material processability and compromise mechanical stability.[26,27] Moreover, the dynamic integration of polarization modulation with multiple luminescence modes remains underdeveloped, which limits the practical implementation of these materials in multidimensional anti-counterfeiting applications. Therefore, constructing composite materials that combine environmental stability, self-healing ability, and a synergistic polarization–multimode luminescence response presents a critical challenge in this field.

In this study, luminescent molecules were encapsulated within polyacrylamide microspheres and incorporated into an AuNR-doped ferric ion-crosslinked hydrogel exhibiting upper critical solution temperature (UCST) behavior (Au-UCST-Fe^{3+}), resulting in a novel luminescent material with triple-emission characteristics. The arrangement and orientation of the local AuNRs were controlled *via* ultraviolet (UV) lithography, enabling the observation of distinct color patterns under different polarization directions. In thicker regions, the transverse localized surface plasmon resonance (TSPR) of the AuNRs enhances the Förster resonance energy transfer efficiency, reduces the fluorescence quantum yield, and induces polarization. In contrast, thinner regions retained the original blue–green emission without significant polarization effects. Moreover, the phosphorescence intensity was modulated through localized humidification. By leveraging the unique features of composite luminescent materials (including polarization, self-healing, humidity responsiveness, and multimodal luminescence [fluorescence, phosphorescence, and thermally activated delayed fluorescence]), optical patterns can be fabricated *via* 3D printing, ultraviolet lithography, and localized imprinting. These approaches have enabled the realization of dynamic encryption and anti-counterfeiting functionalities, thereby offering a novel strategy for the development of next-generation advanced anti-counterfeiting materials.

EXPERIMENTAL

Materials

All chemicals used in this study were of analytical grade and were employed without further purification. Sodium oleate (NaOL, >97.0%), hexadecyltrimethylammonium bromide (CTAB, >98.0%), ammonium persulfate, sodium borohydride ($NaBH_4$, 99%), acrylamide (99%), 2-acryloylamino-2-methyl-1-propanesulfonic acid (98%), 6,9-diamino-2-ethoxyacridine lactate (99%), ethyl alcohol (≥99.7%), 2,2'-azobis(2-methylpropionitrile) (AIBN, 99%), hydrogen tetrachloroaurate trihydrate ($HAuCl_4{\cdot}3H_2O$), polyvinylpyrrolidone (PVP10, K29–32), 2,2,6,6-tetramethyl-4-piperidinol citrate, and methacrylic acid (MAA) were purchased from Macklin. l-Ascorbic acid (BioUltra, ≥99.5%), *N*,*N*'-methylenebisacrylamide (≥99.0%), silver nitrate ($AgNO_3$, >99%), hydrochloric acid (HCl, 37 wt% in water), ferric chloride hexahydrate ($FeCl_3{\cdot}6H_2O$), 3-[dimethyl-[2-(2-methylprop-2-enoyloxy)-ethyl]azaniumyl]propane-1-sulfonate (DMAPS), citric acid monohydrate ($C_6O_6H_8{\cdot}H_2O$), and sodium hydroxide were obtained from Macklin.

Preparation of Polyacrylamide Microspheres

First, 3 g of acrylamide and polyvinylpyrrolidone were mixed in a round-bottom flask containing 21 g of ultrapure water and 11 g of ethanol. Subsequently, 40 mg of 2-acrylamido-2-methyl-1-propanesulfonic acid and 2 mg of *N*,*N*'-methylenebisacrylamide were added to the flask. The flask was then placed on a magnetic stirrer, and the mixture was stirred at 62 ℃ until it was fully dissolved. Once the mixture reached the specified temperature, a solution containing 0.15 g) dissolved in 10 g of ethanol was poured into a flask, and the reaction mixture was stirred continuously for 12 h. After polymerization, the product was centrifuged at 1×10^4 r/min for 10 min to collect the precipitate. The resulting precipitate was oven-dried at 80 ℃ to remove residual solvents, yielding a milky-white solid product of the polyacrylamide microspheres.

Preparation of Luminescent Molecular

First, 1 g of 2-ethoxy-6,9-diaminoacridine lactate monohydrate was dissolved in 100 mL of ultrapure water in a round-bottom flask at 60 ℃. A 10% potassium hydroxide solution was then prepared and added to the flask to induce the formation of the yellow product 2-methoxy-6,9-diaminoacridine. The mixture was centrifuged, and the supernatant was discarded. The resulting precipitate was washed thrice with ultrapure water and subsequently dried in an oven at 80 ℃ to yield a yellow-brown powder.

Preparation of Au-UCST-Fe^{3+} Luminescent Composite

First, 3 g of acrylamide microspheres were dissolved in 7.5 mL of ultrapure water *via* ultrasonic treatment. After complete dissolution, 32 mg of luminescent molecule was added to encapsulate the fluorescent compound within the polyacrylamide microspheres, and stirring was continued until the solution became fully homogeneous. A brown-yellow, clear, and transparent solution was obtained. The Au-UCST-Fe^{3+} hydrogel was successfully synthesized in our previous work;[28] therefore, the detailed preparation process was not repeated here. For specific synthesis details, please refer to the electronic supplementary information (ESI). The Au-UCST-Fe^{3+} luminescent hydrogel was prepared by adding 30 μL of the luminescent solution to the pre-synthesized Au-UCST-Fe^{3+} hydrogel, followed by heating and concentrating the mixture to increase the solid content from 20 wt% to 30 wt%.

Characterization

The sizes of the polyacrylamide microspheres were measured using the particle size analysis mode of a zeta potentiometer (Malvern, UK). The fluorescence decay lifetimes of the samples at 100, 200, and 300 K were recorded using a FLS980 fluorescence spectrometer. Fluorescence quantum efficiency was determined using a Horiba optical instrument. The fluorescence spectrum of the luminescent molecular solution and the fluorescence and absorption spectra of the Au-UCST-Fe^{3+} composite luminescent material were measured using an Ocean Insight marine optical fiber spectrometer with a DH-mini-UV-Vis-NIR

https://doi.org/10.1007/s10118-025-3428-1

light source. A slot between the incident light source and sample holder was used to place a polarizer, which could be rotated to any angle for polarization-dependent measurements. The polarization absorption spectra of the Au-UCST-Fe^{3+} composite luminescent materials along the axis (//), vertical axis (⊥), and non-polarized direction under different degrees of stretching were measured through the adjustment of the light source to the visible light range. The polarized fluorescence spectra of the luminescent molecular solutions and Au-UCST-Fe^{3+} composite luminescent materials in the //, ⊥, and non-polarized directions were recorded under varying stretching conditions in a dark environment. Room-temperature delayed fluorescence spectra of polymer films doped with luminescent molecules encapsulated in polyacrylamide microspheres, as well as those of Au-UCST-Fe^{3+} composite luminescent material films, were measured using an Ocean optical fiber spectrometer set to phosphorescence mode. The light source was a halogen lamp (DH-mini-UV-Vis-NIR) produced by Ocean Optics, and the delay time was set to 8 ms. In addition, using the freezing effect of liquid nitrogen, the delayed fluorescence emission spectrum of the light-yellow luminescent molecular powder encapsulated in polyacrylamide microspheres was tested at low temperature.

RESULTS AND DISCUSSION

Photophysical Properties of Luminescent Molecules

This study demonstrates a multistep synergistic strategy to construct Au-UCST-Fe^{3+} composite luminescent materials (Fig. 1). Building on our previous work, a Au-UCST-Fe^{3+} hydrogel with polarization properties was synthesized through crosslinking reactions between AuNRs and ferric citrate complexes (Fig. 1a).[28] Polyacrylamide microspheres were subsequently prepared *via* the free radical polymerization of acrylamide. The size distribution and morphology of the microspheres (Fig. S1 in ESI) confirmed the uniform particle size and good dispersity of the microspheres. The results showed an average particle size of 100 nm and a polymer dispersity index (PDI) of 0.348. The polyacrylamide microspheres served as encapsulation carriers for the luminescent molecules (Fig. 1b). The luminescent molecule was subsequently encapsulated within the microspheres to protect it from quenching by water and atmospheric oxygen.[29] This composite system exhibited fluorescence, phosphorescence, and thermally activated delayed fluorescence (Fig. 1c). Finally, the microsphere-encapsulated luminescent components were uniformly dispersed throughout the hydrogel, enabling synergistic modulation of both the optical and mechanical properties

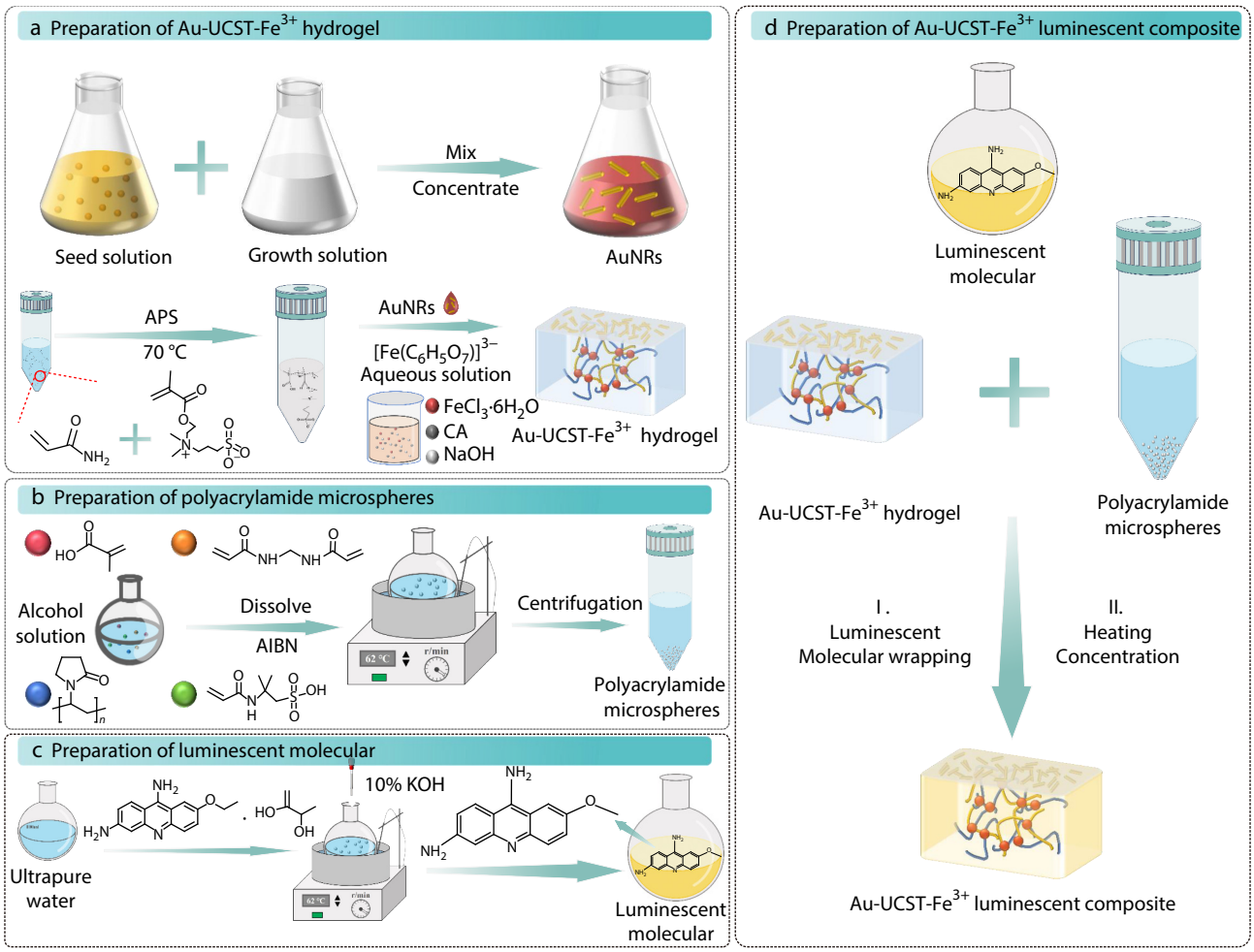

Fig. 1 Construction of the Au-UCST-Fe^{3+} composite luminescent material. (a) Synthesis of the Au-UCST-Fe^{3+} hydrogel; (b) Preparation of polyacrylamide microspheres; (c) Encapsulation of luminescent molecules; (d) Formation of the Au-UCST-Fe^{3+} luminescent composite.

https://doi.org/10.1007/s10118-025-3428-1

(Fig. 1d).

To investigate the influence of polyacrylamide microsphere encapsulation on the photophysical behavior of luminescent molecules, the free molecules and encapsulated composite were analyzed *via* fluorescence and room-temperature delayed fluorescence spectroscopy. The molecular structure of the fluorescent compound is shown in Fig. 2(a). In an aqueous solution, the free luminescent molecule exhibited a prominent emission peak at 497 nm under 365 nm UV excitation (Fig. 2b). Upon encapsulation, the composite system retains a similar fluorescence peak at 495 nm (Fig. 3a). Additionally, its delayed fluorescence spectrum, measured with an 8 ms delay, displayed emission peaks at 500 nm and 610 nm, which were attributed to phosphorescence (Fig. 2c). This slight spectral shift may be attributed to microenvironmental effects introduced by the polymer composites, such as changes in local polarity, hydrogen bonding interactions, and spatial confinement.[30,31] These factors can subtly influence the photophysical behavior of luminescent molecules without fundamentally altering their emission mechanisms. Consequently, the core photophysical properties of the luminescent molecules remained largely preserved following encapsulation within the polyacrylamide microspheres.

Temperature-dependent transient delayed fluorescence spectroscopy was conducted to determine whether the afterglow component of the luminescent molecule arose from delayed fluorescence, phosphorescence, or a combination of both. The results revealed that the intensity of the emission peak at approximately 500 nm increased progressively with increasing temperature, whereas the peak near 610 nm showed minimal variation over time and temperature (Fig. 2d). These observations indicated that the 500 nm peak corresponded to delayed fluorescence, while the 610 nm peak corresponded to phosphorescence emission. This behavior is attributed to the relative stability of triplet excitons and the suppression of the reverse intersystem crossing (RISC) process at low temperatures.[32] However, as the system temperature increased, the RISC was gradually activated. Triplet excitons (T1) are more likely to transition to the S1 state *via* RISC and subsequently relax to the ground state (S_0), resulting in enhanced delayed fluorescence emission. These results confirm that the afterglow of luminescent molecules involves both delayed fluorescence and phosphorescence. To further verify the thermally activated delayed fluorescence (TADF) and phosphorescence characteristics of luminescent molecules, transient lifetime measurements of the microsphere-encapsulated composite system were conducted under vacuum conditions. Considering that TADF compounds exhibit RISC behavior and are highly temperature-sensitive, changes in the exciton lifetime at different temperatures can help distinguish whether the emission arises from TADF or phosphorescence.

At 500 nm, the lifetime decay curve of the luminescent molecule exhibited a downward trend with increasing temperature, indicating a gradual decrease in the delayed fluorescence lifetime (Fig. 2e). This behavior is attributed to the accelerated transition of triplet excitons to the singlet excited state *via* the RISC process facilitated by thermal activation. As a result, the proportion of delayed fluorescence within the total emission increased from 32% to 83%, confirming that the

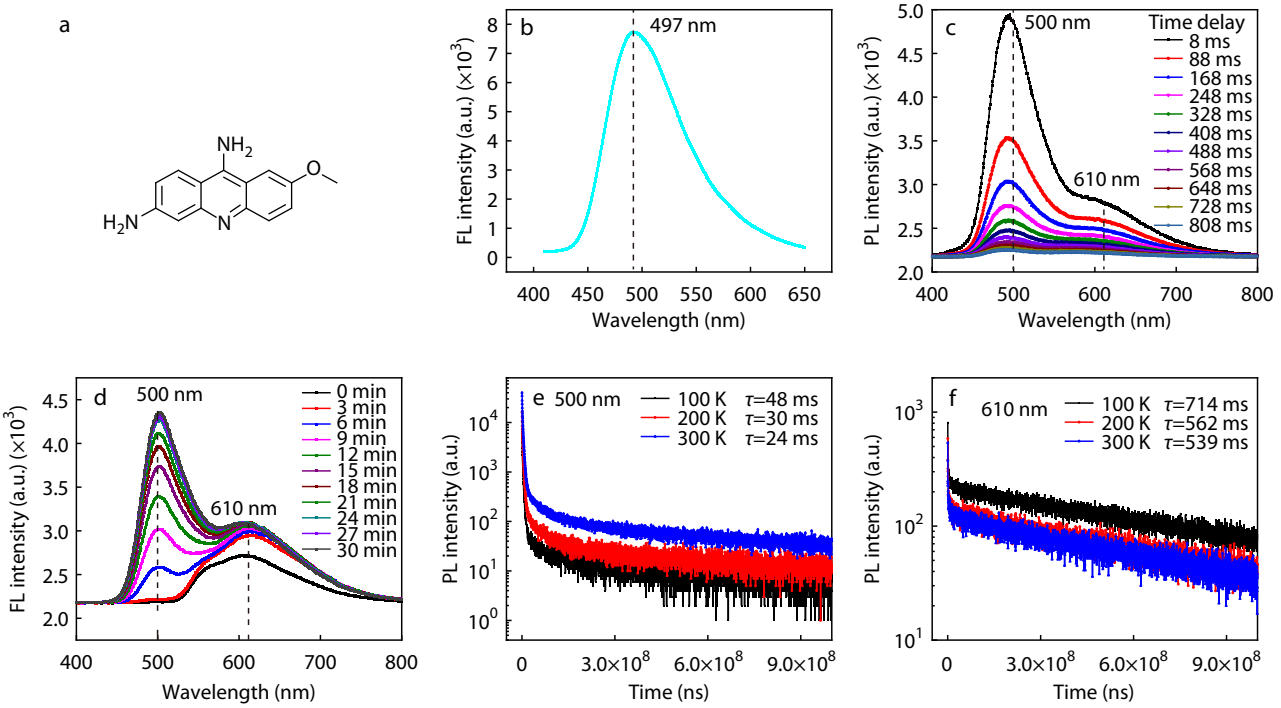

Fig. 2 (a) Molecular structure of the fluorescent compound; (b) Room-temperature photoluminescence spectra of the fluorescent molecule; (c) Room-temperature delayed luminescence spectra of the encapsulated system; (d) Time-dependent delayed phosphorescence spectra of the fluorescent molecule at low temperatures; (e) Transient decay curve of the luminescent molecule at 500 nm; (f) Transient decay curve of the luminescent molecule at 610 nm.

https://doi.org/10.1007/s10118-025-3428-1

500 nm emission originated from TADF and that elevated temperatures promoted RISC. Moreover, the lifetime decay curve at 610 nm declined with increasing temperature (Fig. 2f). This trend was due to an increase in the nonradiative transition rate and a decrease in the proportion of triplet excitons returning to the ground state through phosphorescent emission, resulting in a shortened lifetime.

Photophysical Properties of Au-UCST-Fe^{3+} Composite Luminescent Materials

In our previous work, an AuNR-doped, ferric ion-crosslinked hydrogel with UCST behavior (Au-UCST-Fe^{3+}) was developed.[28] The hydrogel exhibited UV-responsive Fe^{3+}/Fe^{2+} redox cycles and dynamic supramolecular networks. Building on this work, the luminescent molecule was encapsulated within polyacrylamide to construct the Au-UCST-Fe^{3+} luminescent composite. This material not only retained the original properties of polarization, self-healing, and patterning, but also exhibited triple-emission characteristics simultaneously. Subsequently, photoluminescence (PL) spectroscopy was performed on the composite luminescent material to verify that the photophysical properties of the luminescent molecules remained unchanged after incorporation into the composite system (Fig. 3a). According to the results, the emission peak of the composite luminescent material at 495 nm was consistent with that observed in the polyacrylamide microsphere-encapsulated system. This slight shift is attributed to local polarity, hydrogen bonding, and spatial confinement effects following incorporation into Au-UCST-Fe^{3+} composites.[30,31] The consistent peak positions and intensities confirm that the photophysical properties of the luminescent molecules were preserved throughout the doping process. Additionally, the excitation light could penetrate the film to activate luminescent molecules, and the emitted light could pass through the film owing to the high transmittance of the Au-UCST-Fe^{3+} composite. As a result, the Au-UCST-Fe^{3+} composite film exhibited luminescence properties. In phosphorescence mode with a delay time of 10 ms, two emission peaks were observed at 500 nm and 605 nm. The 500 nm peak closely matched the instantaneous fluorescence peak at 495 nm, confirming its origin as delayed fluorescence from the Au-UCST-Fe^{3+} composite. The emission at 605 nm is attributed to phosphorescence. These findings demonstrated that the photophysical properties of the luminescent molecules remained unchanged upon incorporation into the composite material, indicating the inherent stability of their photophysical characteristics.

To investigate the polarized emission retention of the Au-UCST-Fe^{3+} luminescent composite material, PL characterization was conducted at a 300% stretching ratio (Fig. 3b). Under UV excitation, the parallel-polarized fluorescence at 520 nm, corresponding to the TSPR of the AuNRs, exhibited a stronger intensity (Fig. 3c). In contrast, the perpendicular polarization displayed a noticeable dip at this wavelength, indicating fluorescence absorption induced by the TSPR. After the

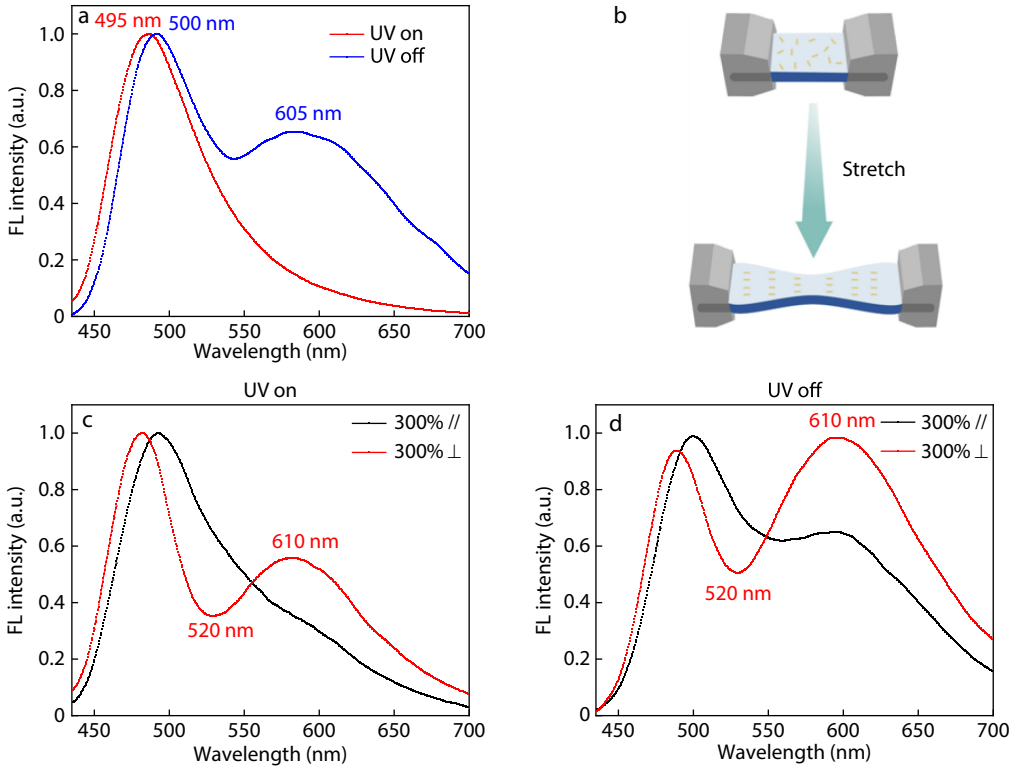

Fig. 3 (a) Room-temperature fluorescence spectrum, delayed fluorescence spectrum, and phosphorescence spectrum of the Au-UCST-Fe^{3+} composite luminescent material; (b) Schematic of the stretched Au-UCST-Fe^{3+} composite luminescent material sample; (c) Polarized fluorescence spectra of the Au-UCST-Fe^{3+} composite luminescent material under 300% tensile strain, measured with polarized light parallel and perpendicular to the stretching direction, respectively; (d) Polarized delayed fluorescence and phosphorescence spectra of the Au-UCST-Fe^{3+} composite luminescent material under 300% tensile strain, measured with polarized light parallel and perpendicular to the stretching direction.

https://doi.org/10.1007/s10118-025-3428-1

UV light was switched off, the composite exhibited delayed fluorescence (500 nm) and phosphorescence (610 nm) emissions under both parallel and perpendicular polarizations relative to the stretching direction (Fig. 3d). Notably, perpendicular polarization again showed a dip at 520 nm, leading to reduced delayed fluorescence and enhanced phosphorescence at 610 nm. These results confirm that the delayed fluorescence and phosphorescence emission characteristics of the composite luminescent material exhibited polarization-dependent behavior, which was influenced by the stretching-induced alignment of the embedded AuNRs.

Polarized Optical Properties of Au-UCST-Fe^{3+} Composite Luminescent Materials

To investigate the strain-dependent polarized emission, photophysical measurements were performed under varying tensile strains. Under natural light, the composite exhibited distinct emission colors when observed through polarized light oriented parallel (//) and perpendicular (⊥) to the stretching direction (Fig. 4a). Under UV illumination, the material emitted cyan fluorescence, which is consistent with the previously reported fluorescence peak (Fig. 4b). Polarized absorption spectra revealed that increasing the tensile strain enhanced longitudinal longitudinal surface plasmon resonance (LSPR) absorption and decreased transverse LSPR absorption when the polarization was aligned parallel to the stretching direction (Figs. 4c and 4d).[33] Conversely, the opposite trend was observed for perpendicular polarization, confirming that stretching induced the alignment of the AuNRs along the direction of strain.[34] Before stretching, the absorption difference was nearly zero, indicating a random orientation of the AuNRs. At a stretching ratio of 300%, the fluorescence intensity difference increases to approximately 0.24, reflecting a gradual enhancement in the alignment of the AuNRs. Similarly, the fluorescence emission near the TSPR peak at 520 nm decreased with increasing strain owing to a reduction in film thickness and a lower AuNR density per unit area.

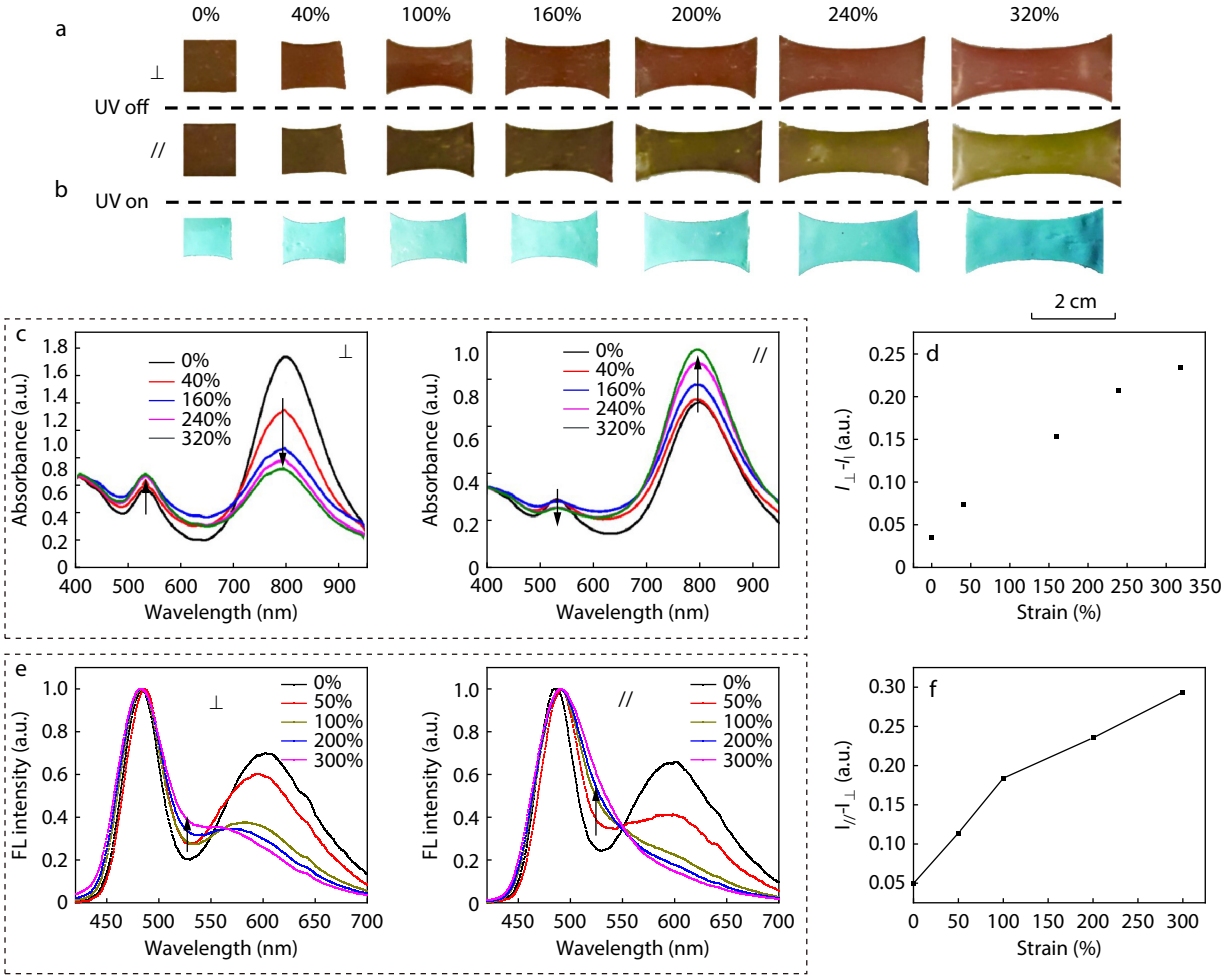

Fig. 4 (a) Photographs of the original and stretched Au-UCST-Fe^{3+} composite luminescent material under polarized light parallel and perpendicular to the stretching direction; (b) Fluorescence color of the Au-UCST-Fe^{3+} composite luminescent material under UV irradiation. Scale bars in (a) and (b) are 2 cm. (c) Fluorescence spectra of the Au-UCST-Fe^{3+} composite luminescent material under polarized light perpendicular and parallel to the stretching direction at different tensile strains; (d) Difference in transverse surface plasmon resonance (SPR) absorption intensity at 520 nm under polarized light perpendicular and parallel to the stretching direction at varying degrees of strain; (e) Fluorescence spectra of the Au-UCST-Fe^{3+} composite luminescent material under polarized light perpendicular and parallel to the stretching direction at different tensile strains; (f) Difference in fluorescence emission intensity at the transverse SPR peak (520 nm) under polarized light parallel and perpendicular to the stretching direction at various stretching degrees.

https://doi.org/10.1007/s10118-025-3428-1

The TSPR absorption of AuNRs was significantly stronger for light polarized perpendicular to the stretching direction than for light polarized parallel to it (Figs. 4e and 4f). Consequently, the fluorescence emission intensity polarized parallel to the stretching direction was substantially greater than that polarized perpendicular to the stretching direction. These findings demonstrate that the polarized luminescence of the composite can be effectively tuned by the degree of AuNR alignment under external strain, thereby offering adjustable polarization properties for advanced anti-counterfeiting applications.

Application of Au-UCST-Fe^{3+} Composite Luminescent Materials in 3D Printing

The 3D printing functionality of the Au-UCST-Fe^{3+} composite luminescent material was explored based on its UCST behavior. The 3D-printed grid consisted of one layer of horizontal lines and another vertical line, with the AuNRs aligned along the respective printing directions. When viewed through a polarizer aligned parallel to the horizontal direction, the horizontal lines exhibited greyish-green hues. The color appearance was reversed when viewed through a polarizer oriented perpendicular to the horizontal direction (Fig. 5a). Under UV light in a dark environment, the grid emitted a bluish-green fluorescence. These results indicate that the pattern printed with the composite luminescent material possessed polarization-dependent properties, and the 3D-printed grid exhibited high structural integrity and excellent mechanical flexibility (Fig. 5b). The 3D-printed pattern consists of one large circle and two small circles. The printed lines of the large circles were oriented horizontally, whereas those of the smaller circles were aligned vertically. The AuNRs in the large circles showed uniform alignment along the horizontal printing direction, whereas those within the smaller circles were aligned vertically (Fig. 5c). A similar phenomenon was observed when the pattern emitted blue-green fluorescence under UV excitation in the dark. When viewed through a polarizer oriented parallel to the horizontal direction, the large circle appeared grayish-green, while the smaller circles appeared red. In contrast, this color pattern was reversed under perpendicular polarization (Fig. 5d).

Au-UCST-Fe^{3+} Composite Luminescent Material UV Lithography Patterning

UV lithography patterning relies on the photoreduction of ferric ions to ferrous ions using UV light in the presence of citric acid. Considering that ferrous ions cannot cross-link with the carboxyl groups (Fig. 6a), this reaction reduces the viscosity of the hydrogel composite. Consequently, the AuNRs within the composite underwent unrestricted Brownian motion, losing their original aligned orientation and thus their polarization performance. In the experiment, the Au-UCST-Fe^{3+} composite luminescent material was stretched to 300%, and a "0123456789" foil mask was partially applied to the sample for patterning. The unmasked regions were then irradiated with UV light for 40 min. The irradiated regions lost their polarization properties, resulting in a uniform coloration across different polarization directions. Subsequently, the mask was removed, and the spline was dried. When the sample was irradiated with a UV lamp in the dark, blue–green fluorescence was observed (Fig. 6b). Placing the UV light beneath the material and observing it through a polarizer aligned parallel and perpendicular to the stretching axis revealed that the numerals displayed gray–red and gray–green hues, respectively (Fig. 6c). These results indicate that the composite luminescent material possesses both fluorescence- and polarization-dependent emission characteristics. with UV lithography, enabling selective elimination of polarization patterning in irradiated regions.

Local Imprinting Patterning of Au-UCST-Fe^{3+} Composite Luminescent Material

The thickness of the material was locally controlled by imprinting to create regions with varying AuNR distributions. In thinner areas, the reduced number of AuNRs led to a decreased fluorescence absorption at the TSPR wavelength. The material was then irradiated from below using UV light with a 365 nm bandpass filter (Fig. 7a). Strong blue–green fluorescence was observed in thin patterned areas when viewed through a polarizer from the surface. In contrast, thicker regions exhibited different colors depending on the angle between the polarization and stretching directions (Fig. 7b). Specifically, the thick regions appeared red when the polarization direction was perpendicular to the stretching direction, and grayish-black when the polarization direction was parallel to the stretching direction. This behavior resulted from the uneven distribution of AuNRs within the material, causing variations in TSPR absorption. The temperature-dependent sol–gel transition and dynamic coordination between Fe^{3+} ions and carboxyl groups endowed the Au-UCST-Fe^{3+} composite with remarkable self-healing capabilities. Lever-

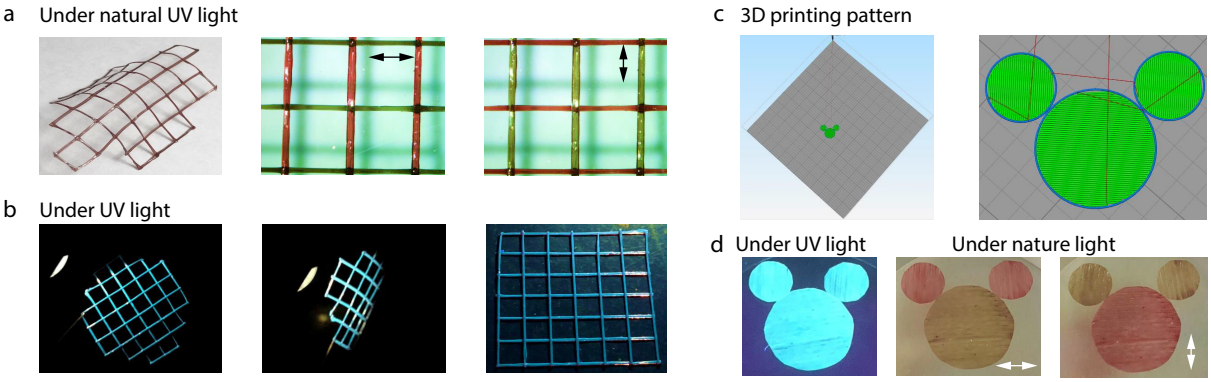

Fig. 5 (a) Polarization images of the Au-UCST-Fe^{3+} composite luminescent material 3D-printed grid under natural light; (b) Images of the Au-UCST-Fe^{3+} composite luminescent material 3D-printed grid under UV light; (c) 3D-printed pattern lines using the Au-UCST-Fe^{3+} composite luminescent material; (d) Fluorescence and polarization images of the pattern under UV and natural light.

https://doi.org/10.1007/s10118-025-3428-1

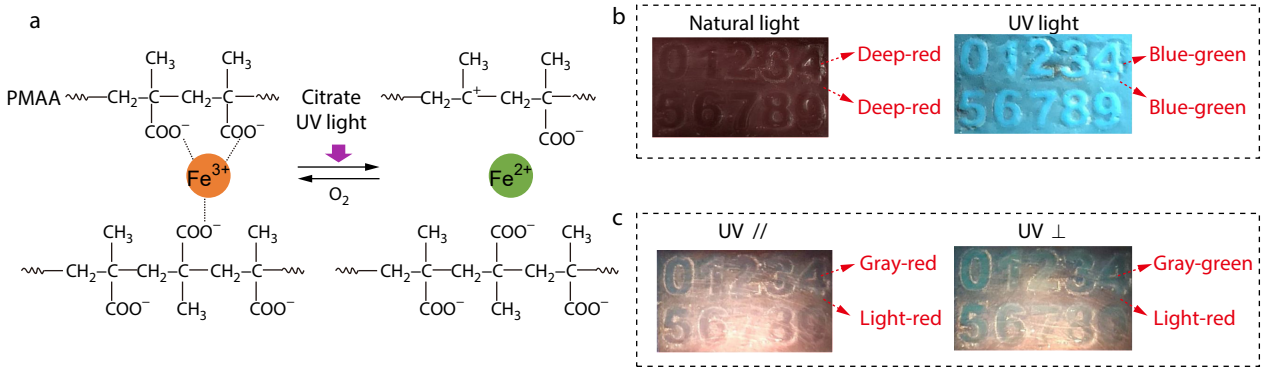

Fig. 6 (a) Schematic of the reaction between iron(III) and carboxyl groups in the presence of citric acid; (b) Images of the numeral pattern under natural light and UV light; (c) Images of the numeral pattern observed under UV light with different polarization directions.

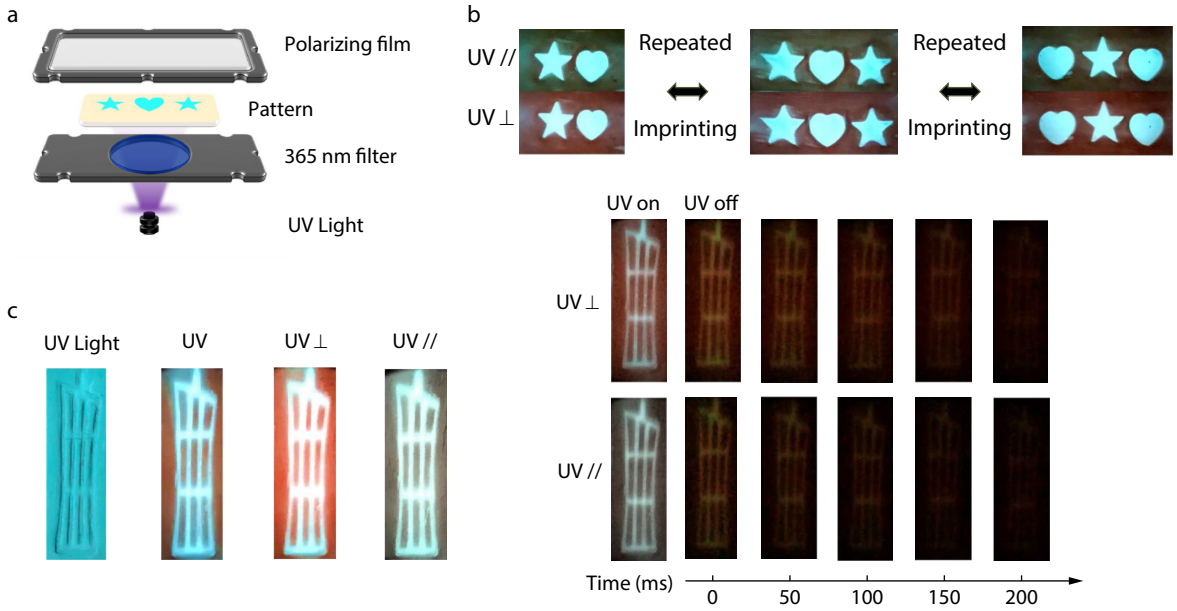

Fig. 7 (a) Schematic of local embossing patterning; (b) Fluorescence polarization patterns of the Au-UCST-Fe^{3+} composite luminescent material; (c) Fluorescence, polarized fluorescence, polarized delayed fluorescence, and polarized phosphorescence images of the embossed "tower" pattern in the Au-UCST-Fe^{3+} composite luminescent material under UV light on/off conditions.

aging these self-healing and reconfigurable properties, we designed reversible "star" and "heart" patterns.[28] Following simple compression molding followed by thermal recovery, the material behaved like remoldable rubber clay, retaining distinct patterns after each molding cycle, while remaining easily reshaped. Consequently, it can reversibly switch between the "star" and "heart" configurations through repeated pressing and heating. First, the "star" and "heart" patterns were formed by pressing. Pressing again allowed the addition of a new "star," transforming the pattern into a "star–heart–star" configuration. After heating, the material returned to its original state, and pressing again produced a "heart–star–heart" pattern. This finding demonstrates that the Au-UCST-Fe^{3+} composite luminescent material enables repeatable polarization fluorescence patterning. Similarly, the region-selective water-induced quenching strategy yielded comparable results (Fig. S2 in ESI).

Similarly, the composite luminescent material exhibited polarized delayed fluorescence and polarized phosphorescence, which enabled additional fluorescence polarization patterning. A "tower" pattern was designed for subsequent experiments (Fig. 7c). When UV light was illuminated from beneath the material, only thin regions of the tower emitted blue–green fluorescence. When viewed through a polarizer with a polarization direction perpendicular to the stretching axis, the thick regions appear red. In contrast, with the polarization parallel to the stretching direction, the thick regions appeared grayish-black. Under UV light and perpendicular polarization, the tower displayed blue–green fluorescence, whereas the surrounding area appeared red. After the UV light was switched off, the tower exhibited gradually fading delayed fluorescence and phosphorescence, which remained faintly visible, whereas the surrounding regions darkened. This finding demonstrates that the delayed fluorescence and phosphorescence of the tower were stronger than those in other areas. When the polarization direction was parallel to the stretching axis, the tower exhibited blue–green fluorescence, whereas the surrounding regions appeared grayish-black. Similarly, turning off the UV light produced fading ef-

https://doi.org/10.1007/s10118-025-3428-1

fects consistent with those observed in the perpendicular polarization direction. This behavior is attributed to the thinner regions of the tower pattern containing fewer AuNRs, resulting in less absorption of the delayed fluorescence and phosphorescence. Consequently, the tower remained visible for a longer time after UV light was turned off.

CONCLUSIONS

A luminescent molecule was designed and incorporated into a previously synthesized Au-UCST-Fe^{3+} composite to prepare the Au-UCST-Fe^{3+} composite luminescent material. This material exhibits fluorescence, TADF, and phosphorescence emission characteristics. The results showed that The luminescent properties remained unaffected after the Au-UCST-Fe^{3+} hydrogel was doped with luminescent molecules. In addition, the composite retained its self-healing and patterning capabilities. Under UV excitation, the energy emitted by the luminescent molecule was absorbed by the AuNRs *via* the TSPR effect. Moreover, by varying the stretching degree and extrusion orientation of the Au-UCST-Fe^{3+} composite luminescent material, the arrangement of the AuNRs within the composite could be modified, thereby endowing the system with polarized emission characteristics. Based on these material properties, UV lithography and local imprinting techniques have been employed to achieve patterning. In the UV lithography process, a plate template is used for local masking, followed by UV lamp irradiation. The irradiated regions caused the AuNRs to lose their ordered orientation, while the AuNRs in the unexposed areas retained their original alignment. This selective disruption enabled controlled depolarization in the exposed regions and maintained the polarization in the masked areas, thereby creating distinct patterns. Local imprinting was employed to vary the AuNR content by controlling the material thickness, producing differential TSPR effects that modulated the fluorescence absorption of luminescent molecules. This thickness-dependent modulation enabled the creation of distinct fluorescence patterns in regions with varying thicknesses. In the thick regions, fluorescence was absorbed by the AuNRs *via* the TSPR effect, and the emitted fluorescence was polarized, whereas the thin regions retained blue–green fluorescence with less pronounced polarization. Additionally, dynamic fluorescence patterning was achieved under UV excitation through the local adjustment of humidity levels via targeted humidification. This study offers a novel approach for the functional application of Au-UCST-Fe^{3+} composite luminescent materials in optical anti-counterfeiting.

Conflict of Interests

The authors declare no interest conflict.

Electronic Supplementary Information

Electronic supplementary information (ESI) is available free of charge in the online version of this article at http://doi.org/10.1007/s10118-025-3428-1.

Data Availability Statement

The data that support the findings of this study are available from the corresponding author upon reasonable request. The author's contact information: lushlin@gdut.edu.cn.

ACKNOWLEDGMENTS

This work was financially supported by the National Key R&D Program of China (No. 2023YFB3812400) and the National Natural Science Foundation of China (Nos. 52203353 and 52433004).

REFERENCES

1 Sun, L.; Wang, B.; Xing, G.; Liang, C.; Ma, W.; Yang, S. Bi-Induced Photochromism and photo-stimulated luminescence with fast photochromic response for multi-mode dynamic anti-counterfeiting and optical information storage. *Chem. Eng. J.* **2023**, *455*, 140752.

2 Shen, Y.; Le, X.; Wu, Y.; Chen, T. Stimulus-responsive polymer materials toward multi-mode and multi-level information anti-counterfeiting: recent advances and future challenges. *Chem. Soc. Rev.* **2024**, *53*, 606–623.

3 Liu, J.; Ji, Y.; Liu, X.; Omoniyi, A. O.; Mingda, Y.; Liang, Q.; Chen, D.; Zhou, Y.; Zhang, J.; Su, Z. 4D encryption system: hydrophilic-hydrophobic polyurethane actuators with smart color switching for high-capacity data storage. *Adv. Funct. Mater*. **2025**, *2501801*.

4 Chen, Z.; Yang, J.; Xu, R.; Zhao, Z.; Sang, X.; Liu, L.; Feng, M.; Song, F.; He, Y.; Huang, W. Programmable broadband responsive lanthanide-doped nanoarchitecture for information encryption. *Adv. Opt. Mater.* **2022**, *10*, 2101843.

5 Shi, Y.; Han, J.; Jin, X.; Miao, W.; Zhang, Y.; Duan, P. Chiral luminescent liquid crystal with multi-state-reversibility: breakthrough in advanced anti-counterfeiting materials. *Adv. Sci.* **2022**, *9*, 2201565.

6 Hua, Y.; Huang, L.; Shen, Y.; Huang, K.; Cui, W.-B.; Li, Z.-Y.; Zhang, H. Photofluorochromic organic supramolecular compounds for multiple dynamic anticounterfeiting. *Inorg. Chem. Front.* **2024**, *11*, 8350–8358.

7 Oh, J. W.; Lee, S.; Han, H.; Allam, O.; Choi, J. I.; Lee, H.; Jiang, W.; Jang, J.; Kim, G.; Mun, S.; Lee, K.; Kim, Y.; Park, J. W.; Lee, S.; Jang, S. S.; Park, C. Dual-light emitting 3D encryption with printable fluorescent-phosphorescent metal-organic frameworks. *Light Sci. Appl.* **2023**, *12*, 226.

8 Wu, B.; Xu, X.; Tang, Y.; Han, X.; Wang, G. multifunctional optical polymeric films with photochromic, fluorescent, and ultra-long room temperature phosphorescent properties. *Adv. Opt. Mater*. **2021**, *9, 2101266*.

9 Tang, M.; Wen, J.; Sun, Y.; Hou, Q.; Cai, X.; He, W.; Xie, X.; Ding, H.; Li, F.; Zheng, L.; Shi, Y.; Cao, Q. Organic chameleon: fluorescence, phosphorescence and radical afterglow triple emission from naphthylimide functionalized tri-phenylphosphine derivatives. *Adv. Funct. Mater.* **2024**, *34*, 2314130.

10 Zhao, D.; Li, X.; Li, Q.; Yue, C.; Wang, Y.; Li, H. Self-healing photoluminescent polymers with photosensitive behavior for information storage and multiple-level dynamic encryption. *Chem. Sci.* **2024**, *15*, 13306–13312.

11 Lu, L.; Wang, K.; Wu, H.; Qin, A.; Tang, B. Z. Simultaneously achieving high capacity storage and multilevel anti-counterfeiting using electrochromic and electrofluorochromic dual-functional AIE polymers. *Chem. Sci.* **2021**, *12*, 7058–7065.

12 Jin, P.; Wei, X.; Yin, B.; Xu, L.; Guo, Y.; Zhang, C. Stepwise charge/energy transfer in MR-TADF molecule-doped exci-plex

for ultralong persistent luminescence activated with visible light. *Adv. Mater.* **2024**, *36*, 2400158.
13 Chen, J.; Zhang, X.; Xie, Z.; Liu, B. Ultralong thermally acti-vated delayed fluorescence based on intermolecular charge transfer induced by isomer in carbazole derivative. *Aggregate* **2024**, *5*, e638.
14 Jin, L.; Chen, J.; Sun, J.; Mo, W.; Zheng, Y.; Hong, W. Photo-controllable persistent luminescence in doped polymers for reversible high-resolution patterning and multiple stimuli-response. *Adv. Opt. Mater.* **2024**, *12*, 2301514.
15 Huang, L.; Liu, L.; Li, X.; Hu, H.; Chen, M.; Yang, Q.; Ma, Z.; Jia, X. Crystal-state photochromism and dual-mode mechanochromism of an organic molecule with fluorescence, room-temperature phosphorescence, and delayed fluorescence. *Angew. Chem. Int. Ed.* **2019**, *58*, 16445–16450.
16 Maillard, J.; Klehs, K.; Rumble, C.; Vauthey, E.; Heilemann, M.; Fürstenberg, A. Universal quenching of common fluorescent probes by water and alcohols. *Chem. Sci.* **2021**, *12*, 1352–1362.
17 Li, T.; Zhang, N.; Zhao, S.; Liu, M.; Zhang, K.; Zhang, C.; Shu, J.; Yi, T.-F. Long-lived dynamic room temperature phosphorescent carbon dots for advanced sensing and bioimaging applications. *Coord. Chem. Rev.* **2024**, *516*, 215987.
18 Yang, L.; Liang, X.; Wang, Z.; Zhang, Q.; Wang, S.; Liang, X.; Xu, Y.; Zhang, Y.; Yin, Y. Regulating the aggregation and dispersion of carbon dots to achieve stimulus-responsive multimodal luminescence for dynamic anti-counterfeiting. *Adv. Opt. Mater.* **2025**, *13*, 2402456.
19 Duan, H.; Zhao, J.; Li, S.; Qi, D.; Li, J. Flexible anti-counterfeiting circularly polarized luminescent elastomer from supramolecular polyurethanes. *Adv. Opt. Mater.* **2024**, *12*, 2400379.
20 Dai, M.; Zhou, B.; Fang, X.; Yan, D. Two-dimensional hybrid perovskitoid micro/nanosheets: colorful ultralong phosphorescence, delayed fluorescence, and anisotropic optical waveguide. *ACS Appl. Mater. Interfaces* **2022**, *14*, 40223–40231.
21 Jussila, T.; Pekkanen, J.; Virta, A.; Ghazy, A.; Lastusaari, M.; Karppinen, M. In situ growth of ultrathin Y_2O_3 capping layers for eu-organic thin films *via* atomic/molecular layer deposition. *J. Vac. Sci. Technol. A* **2025**, *43*, 022406.
22 Zhao, X.; Zhou, X.; Cheng, Q.; Liu, Y. Blue phosphorescent solid supramolecular assemblies between hydroxypropyl-*β*-cyclodextrin and triazine derivatives for achieving multicolor delayed fluorescence. *Nano Today* **2025**, *60*, 102561.
23 Huang, S.; Wu, Y.; Hu, Y.; Wang, X.; Yuan, Y.; Zhang, H. Photothermal response and precise control of circularly polarized luminescence via double-layered films based on cholesteric liquid crystals. *J. Mater. Chem. C* **2025**, *13*, 66416649.
24 Zou, R.; Jin, L.; Zheng, Y.; Shao, G.; Hong, W. Chromatically polarized afterglow: photo-controlled and anisotropic persistent luminescence from doped polymeric systems. *Chem. Eng. J.* **2024**, *479*, 147792.
25 Sha, J.; Lu, H.; Zhou, M.; Xia, G.; Fang, Y.; Zhang, G.; Qiu, L.; Yang, J.; Ding, Y. Highly polarized luminescence from an AIEE-active luminescent liquid crystalline film. *Org. Electron.* **2017**, *50*, 177–183.
26 Wu, X. Linearly polarized electroluminescence from ionic iridium complex-based metallomesogens: the effect of aliphatic-chain on their photophysical properties. *J. Mater. Chem. C* **2018**, *6*, 3298.
27 Gong, W.; Huang, G.; Zhou, M.; Fan, C.; Yuan, Y.; Zhang, H. Synthesis and properties of room-temperature phospho-rescent liquid crystal copolymers with linearly polarized luminescence characteristic. *ACS Appl. Mater. Interfaces* **2023**, *15*, 49701–49711.
28 Xu, L.; Feng, Y.; Yu, D.; Zheng, Z.; Chen, X.; Hong, W. Recoverable photolithographic patterning for polarized display and encryption. *Adv. Mater. Technol.* **2020**, *5*, 2000373.
29 Chen, Y.; Zhu, X.; Liu, H.; Sun, B. Multi-confinement structured carbon dots with long room temperature phosphorescence lifetime and efficiency for sensing thiram residues assisted by copper ions. *Microchim. Acta* **2024**, *191*, 655.
30 Liu, J.; Li, Z.; Hu, T.; Wei, X.; Wang, R.; Hu, X.; Liu, Y.; Yi, Y.; Yamada-Takamura, Y.; Wang, Y.; Wang, P. Experimental evidence for "hot exciton" thermally activated delayed fluorescence emitters. *Adv. Opt. Mater.* **2019**, *7*, 1801190.
31 W. Zhou, G. Wen, K. Li, H. Xiong, J. Zhang, S. Lu, X. Chen. Room temperature phosphorescence of heavy atom-free indole carboxylic acid/polyacrylamide: low cost, long lifetime and good luminescent efficiency. *Dyes Pigm.* **2022**, *205, 110481*.
32 R. Feng, M. Wang, Z. Zhang, P. Hu, Z. Wu, G. Shi, B. Xu, H. Liu, L. Ma. Polymer-based long-lived phosphorescence materials over a broad temperature based on coumarin derivatives as information anti-counterfeiting *ACS Appl. Mater. Interfaces* **2023**, *15, 30717*.
33 Zhang, H.; Zhang, J.; Tong, X.; Ma, D.; Zhao, Y. Light polarization-controlled shape-memory polymer/gold nanorod composite. *Macromol. Rapid Commun.* **2013**, *34*, 1575–1579.
34 Turner, J. G.; Og, J. H.; Murphy, C. J. Gold nanorod impact on mechanical properties of stretchable hydrogels. *Soft Matter* **2020**, *16*, 6582–6590.

https://doi.org/10.1007/s10118-025-3428-1